Chalcogenide Letters Vol. 20, No. 11, November 2023, p. 759 - 777

Effect of Cu ratios dopant on ZnSe thin films structural and optical properties

M. N. Abdel-Salam[a], N. Sabry[b], E. S. Yousef[c,d], E. R. Shaaban[a,*]
[a]*Department of Physics, Faculty of Science, Al-Azhar University, Assiut 71542, Egypt*
[b]*Nanoscience Laboratory for Environmental and Biomedical Applications (NLEBA), Nuclear Lab., Department of Physics, Faculty of Education, Ain Shams University, Roxy, 11757 Cairo, Egypt.*
[c]*Research Center for Advanced Materials Science (RCAMS), King Khalid University, Abha 61413, P. O. Box 9004, Saudi Arabia*
[d]*Physics Dep., Faculty of Science, King Khalid University, P. O. Box 9004, Abha, Saudi Arabia*

This study focused to prepare poly-crystalline $(ZnSe)_{1-x}$ Cu_x thin films, where *x* values vary from 0 to 0.1 %. the effect of Cu ratios dopant on structural, phases and optical properties has been investigated. As prepared thin films were deposited onto a cleaning glass substrate under high vacuum conditions (10^{-7} mbr) at room temperature using the " evaporation technique". The analysis results according to data of the X-ray diffraction technique of all films refer to the growth polycrystalline with hexagonal wurtzite structure of Zn-Se with no presence of any further phases. The changes in numerous parameters such as volume of the unit cell, atomic packing factor, dislocation density, lattice constant and bond length with the Cu ratio were estimated and described. As well, the crystallite sizes,*D*, the lattice micro-strain,ε and dislocation density,δ have been calculated the results evidence that the micro-structural parameters enhancement with increment Cu atoms. On the other hand, the optical parameters of the as-synthesized films $(ZnSe)_{1-x}Cu_x$ ($0 \leq x \leq 0.1$) were performed utilizing "UV–V is spectro -photometer" with a wavelength range of 300 to 2400 nm. The results show that as the Cu ratio increases, the absorption edge shifts to a higher wavelength and the optical band gap, E_g^{opt} decreases from 2.63 eV to 2.52 eV. Finally, the behaviour of the optical constant parameters as real,ε_r/ imaginary, ε_i parts, dissipation factor,*tan* δ, volume/surface energy loss functions and dispersion parameters were shown to depend on the variation of the Cu ratio and wavelengths.

(Received August 7, 2023; Accepted November 1, 2023)

Keywords: $(ZnSe)_{1-x}Cu_x$, Thin films, X-ray diffraction, Structural parameters, Optical characterization

1. Introduction

Gained semi-conductors materials of the groups II–VI considerable interest due to their unique opt-electronic characteristics and numerous applications in devices [1, 2]. Zn-Se is one of the important material has been rapidly developed and widely, has a direct band-gap of (2.7 eV at RT) which can be utilized of many possibility in devices of applications, for example laser diodes[3], light emitting diodes[4], short lasers wavelength and solar cells, etc.[5-8]. However, there remain a lot of issues with these un-doped Zn-Se films that need to be fixed. To dissolve these troubles, presently, a doping with transition metal impurities as Cu, Mn, Sn, Cd, Er and etc. into Zn-Se films are a significant strategy for enhancing the characteristics, broaden range of absorption spectrum and narrow its energy band-gap which leads to rise the photo-absorption coefficient of un-doped Zn-Se films [9, 10]. On the other hand, introduced an intermediary impurity in band gap (represented in fig.1), there are two methods to produced the electron hole-

* Corresponding author: esam_ramadan2008@yahoo.com
https://doi.org/10.15251/CL.2023.2011.759

pairs, the first one the electrons transmit from the valence-band (V.B) to the intermediary band, after then to the conduction- band (C.B); and the second way the electrons transmit straight from the (V.B) to (C.B), thus, its equivalent to the parallel link of three semi- conductors through various band-gaps, which would significantly increase a material's photo-absorption efficiency [11-15]. The Cupper (Cu) is among of the most interesting materials because it has electronic-shell structure and a similar ionic-radius of Zn^{2+}, thus, thought to be more suitable for Zn^{2+} ion replacement compared toward others [16]. Actually, Se- Zn thin films doped with Cu are the utmost promising electrical- conductivity controlled metal owing to its changeable electrical conductance[17]. Moreover, the composition of Se-Zn doped with Cu is of available elements and low-cost. Likewise, it has considerable potential production as a material for solar absorbers[18] Various methods have been employed to produce Se-Zn doped with Cu films, inclusive the "vacuum evaporation", "the ultrasonic spray-pyrolysis technique", "magnetron sputtering" and "chemical vapor deposition" etc[19-22]. One of these technologies, the "vacuum evaporation" is very important common because of inexpensive fee, reproducibility, and flexibility to deposition on wide area of substrate, as well, the films made with this technique are very homogenous and highly adherent[2].

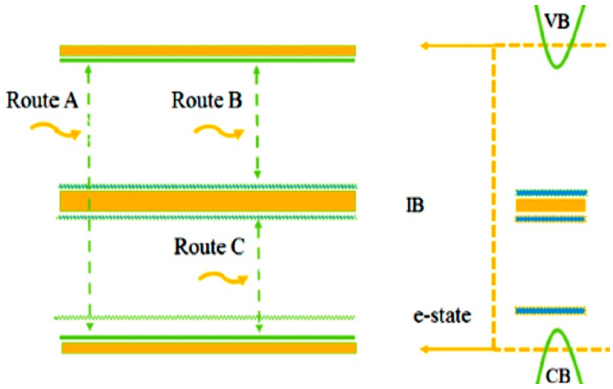

Fig. 1. The model of intermediate band structure.

The goal of this research is to study the morphological characteristic and structural of polycrystalline thin films for $(ZnSe)_{1-x}Cu_x$ $(0 \leq x \leq 0.1)$ are synthesized via the evaporation technique. Through "Scanning Electron Microscopy (SEM)" and "X-ray diffraction" technique were done to identify the structural changes caused by the doped of Cu in Zn-Se films. In addition, the optical characterization of the as-synthesized films were performed utilizing "UV–Vis spectro-photometer" with a wavelength range of 300 to 2400 nm. The variation of energy gap and derived optical parameters are demonstrated according to the micro-structure parameters.

2. Experimental techniques

Bulk alloys of $(ZnSe)_{1-x}Cu_x$ $(0 \leq x \leq 0.1)$ were fabricated using the melt-quenching technique. The amount of Ze, Se, and Cu highly purity chemical components 99.999% (Aldrich Chem Co., USA) according to required atomic ratios were placed in quartz ampoules with "lengths of 8 cm and internal diameters of 8 mm". The sealed ampoules are then heated for 24 hours at 1400 K in an oscillating heater. To guarantee the homogeneity of the alloys the furnace is neatly oscillated round a horizontal axis to shake the melt. At finally of heating duration, the ampoules were quickly quenched in cooled solution. On the other hand, the as-prepare films of (ZnSe)100-xCux $(0 \leq x \leq 10)$ were synthesized using thermal evaporation technique by a coating unit (DV - 502A; Denton Vacuum, Cherry Hill, NJ, USA) under high vacuum conditions (10^{-7} mbr). The substrates for deposition were completely cleaned with an ultrasonic hot bath of distilled water, followed by pure alcohol. The structural examination of both pure thin films of ZnSe and doped with Cu was conducted using the X-ray mechanism "(XRD Philips 1710)". SEM was applied to

analysis the surface morphology of the films, whereas the dispersive energy x-ray spectrometer was utilized to determine their elemental composition (EDS). Finally, the optical properties of the as-prepare films was performed utilizing "UV–V is spectro -photometer" with a wavelength range of 300 to 2400 nm.

3. Results and discussion

3.1. X-ray characterization

The crystalline phases of the thin films of pure ZnSe and doped with Cu according to experimentally XRD diffraction are clear in fig.2. One can see that all films are polycrystalline having a hexagonal structure phase (JCPDS card # 00-015-0105)[23]. The favourably orientation of ZnSe was shown to be grown along the (002) plane with greater intensity than the other two peaks related to the planes (110) and (112). Further, the results showed no essential changes in peak positions for varied doping ratios of Cu: ZnSe films, which means the Cu ion was successfully incorporated into ZnSe alloys without affecting the crystal structure[24, 25]. Notably, fig. 3 shown the alteration in peak intensities for the (002) plane, it is observed with a rise the Cu^{2+}ratio the intensity peak decrease, this may be attributed to inhibit the crystallinity lattice of ZnSe because of the replacement of Zn^{2+} ions with Cu^{2+}ions[24, 25]. In addition, It is probable that incorporation of Cu^{2+} induced a compressive stress on the crystal lattice of the ZnSe causing in the peak position shifts towards a higher angles[26].

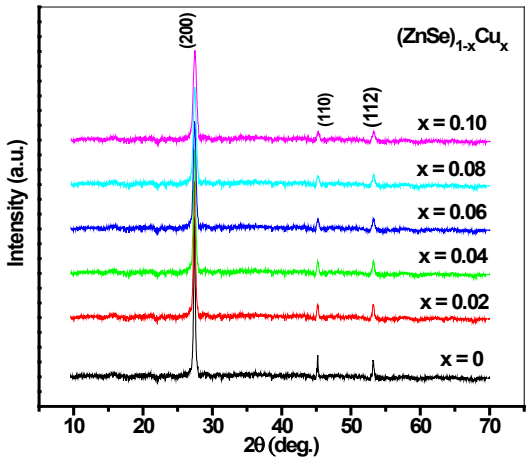

Fig. 2. Patterns of XRD of $(ZnSe)_{1-x}Cu_x$ ($0 \leq x \leq 0.1$) thin films.

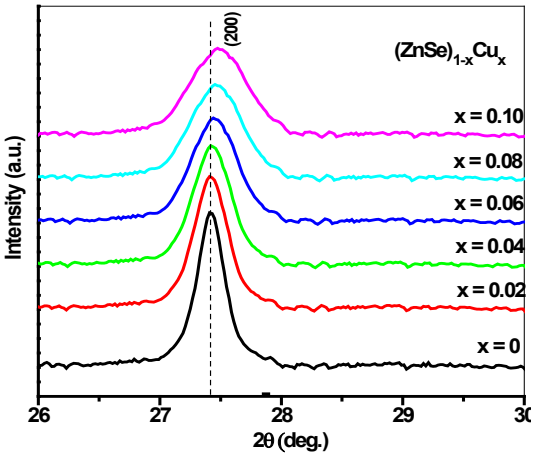

Fig. 3. The comparison of (002) diffraction plan of pure ZnSe and doped with Cu ratio.

In order to understand more about of structural changes in the films under investigation, the values of the "lattice parameters a and c" of the hexagonal ZnSe structures at first order n=1 were evaluated based on the next eqs.

$$a = \frac{\lambda^2}{\left(\sqrt{3}\sin\theta\right)} \tag{1}$$

$$c = \frac{\lambda}{\sin\theta} \tag{2}$$

The results of the calculated values of lattice structural parameters "a" and "c" for pure ZnSe film are a good match in comparison to the typical values of ZnSe single crystals (a=3.9960 Å and c=6.5500 Å)[27, 28]. While it was observed that the estimated values of their "a" and "c" parameters for doped films with Cu ion are reduced with rising Cu ratio, the results emphasizes the occurrence of a compressional stress in the films[29]. Also, the c/a parameter ratio is close to 1.688, indicating that the wurtzite structure shape of pure ZnSe and doped ZnSe/Cu films is reasonably perfect. The obtained values of parameters "a", "c" and c/a are summarized in Table 1 and shown in fig. 4 .

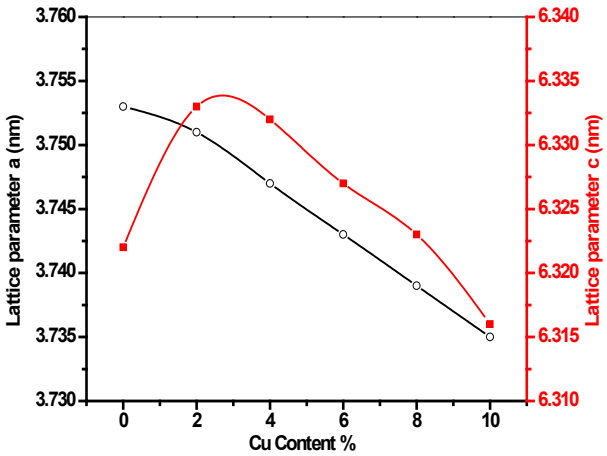

Fig. 4. The lattice parameters,"a" and "c" of $(ZnSe)_{1-x}Cu_x$ $(0 \le x \le 0.1)$ thin films.

Table 1. Structural parameters, volume of unit cell, packing factor , X-ray density and the micro-structural parameters(the crystallite sizes,(D), the lattice micro-strain,(ε) and dislocation density,δ) respectively, of $(ZnSe)_{1-x}Cu_x$ thin films.

Conc. x %	a (nm)	c (nm)	c/a	V $(Å)^3$	P	ρ (g/cm^3)	D (nm)	ε x 10^{-2}	δ x 10^{-3} $(lin/nm)^{-2}$
0	3.7525	6.322	1.6847	77.0966	71.7739	3.5056	21.9128	0.69704	2.0826
2	3.7513	6.3327	1.6881	77.1775	71.6295	3.502	18.749	0.81439	2.8447
4	3.7473	6.3323	1.6898	77.007	71.5575	3.5097	16.4463	0.92743	3.6971
6	3.7433	6.3274	1.6903	76.7832	71.536	3.5199	15.0791	1.0104	4.3979
8	3.7393	6.3226	1.6908	76.5603	71.5144	3.5302	14.1025	1.0793	5.0282
10	3.7353	6.3158	1.6908	76.3153	71.5144	3.5415	13.7686	1.1042	5.275

According to the values of lattice structural parameters "a" and "c" the volume of the unit cell was determined employing eq.3.

$$V = \frac{\sqrt{3}}{2} c^2 a \tag{3}$$

It is clear that, the values of Cu-doped ZnSe films are reduced with an increase in the Cu ratio. This may be due to the reduced values of parameters "a" and "c" and the influence of Cu^{2+} ions into the host structure. The atomic packing factor (APF) of hexagonal was estimated via the formula[30].

$$P = \frac{2\pi a}{3c\sqrt{3}} \tag{4}$$

It is notable that the calculated APF is slightly decreases with a rising in Cu ratio. Also, the values are similar at the 8 % and 10% of Cu dopant. which may be attributed to decreasing the voids of the as-synthesized $ZnSe_{1-x}Cu_x$ films, which demonstrates a uniform replacement of Cu ions in the zinc positions of the ZnSe structure [24, 29]. The obtained values of the volume unit cell and (APF) are listed in table 1. On the other hand, the density,, of pure films Znse and doped with Cu^{+2} ions can also be determined through the following formula.

$$\rho = \frac{nM}{N_A V} \tag{5}$$

It has been discovered that the density of $(ZnSe)_{1-x}Cu_x$ ($0 \leq x \leq 0.1$) thin films increases with increasing Cu ratio. It might be attributed to the reduction of the molecular weight "molecular weight of Cu^{+2} (63.546 amu) ions is smaller than that of Zn^{+2} (65.38 amu) ions" and unit cell volume[31]. The obtained values of density are clearly in table 1. In addition, the crystallite sizes,(D) and the lattice micro-strain,(ε) of the thin films under study can be calculated according to Debye-Scherrer's eqs. (6 and 7), respectively[32, 33].

$$D = \frac{K\lambda}{\beta \cos\theta} \tag{6}$$

$$\varepsilon = \frac{\beta}{4\tan(\theta)} \tag{7}$$

where K is the Scherrer factor, which is typically equal to 0.94, and β is the full width of half maximum peak's (FWHM). The dislocation density, can be also computed used to the next Formula[34].

$$\delta = \frac{1}{D^2} \tag{8}$$

The computed values of D, ε and δ for $(ZnSe)_{1-x}Cu_x$ ($0 \leq x \leq 0.1$) films under examination are listed in table2. It is evident that the crystallite size,D decrease while both the micro-strain,ε and dislocation density,δ raise with increment Cu^{+2} ion into the host Znse lattice. Fig.5 demonstrates alteration the lattice structure parameters D, ε and δ as a function of the variating Cu^{+2} ratio inside ZnSe host lattice.

.

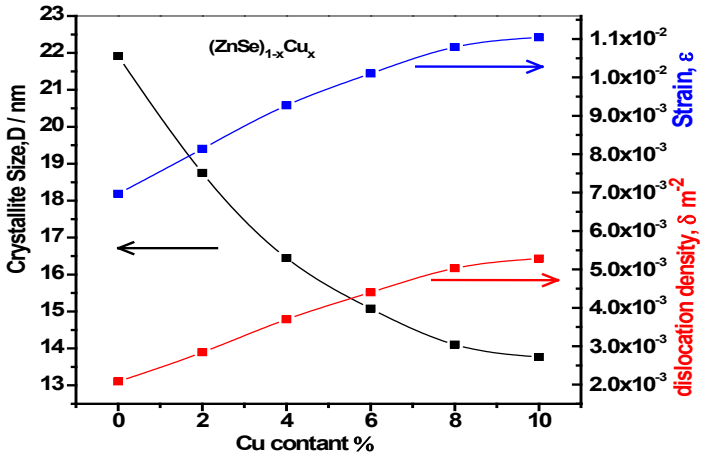

Fig. 5. The dependence of the micro-structural parameters D, ε and δ on the variation of the Cu ratio.

Table 2. Potential parameter, bond length, sec nearest neighbor bond length, one along c-direction, ec nearest neighbor bond length six along c-direction, sec nearest neighbor bond length three along c-direction and both bond angle for $(ZnSe)_{1-x}Cu_x$ thin films.

Conc. x %	u	*L* (Å)	b_1' (Å)	b_2' (Å)	b_3' (Å)	α (°)	β (°)
0	0.3674	0.2323	0.3999	0.4413	0.4413	111.1473	107.7444
2	0.367	0.2324	0.4009	0.4413	0.4413	111.2548	107.6302
4	0.3667	0.2322	0.401	0.4409	0.4409	111.3085	107.5731
6	0.3667	0.232	0.4007	0.4404	0.4404	111.3246	107.5559
8	0.3666	0.2318	0.4005	0.4399	0.4399	111.3407	107.5388
10	0.3666	0.2315	0.4	0.4395	0.4395	111.3407	107.5388

The behaver observed may be attribute to the change in the size of lattice as a result of vacancies created with Cu substitution inside ZnSe lattice, leading to lattice distortion [40], consequently baseness of crystallinity. This indicates that existence tensile micro-strain included into the ZnSe lattice[7, 35]. as well, arising donor sites could be the cause of the rising dislocation density and strain with increased Cu ratio[36]. On the other hand, the length of bond, l was obtained from the formula [37]

$$l = \sqrt{\frac{a^2}{3} + c^2\left(\frac{1}{2} - u\right)^2} \tag{9}$$

where u is described as just a positional parameter of the wurtzite structure, obtained by

$$u = \frac{a^2}{3c^2} - 0.25 \tag{10}$$

It is noticed that the calculated values for the bond length of thin films under examined were slightly changed. This may be due to the change in the electronegativity between Cu and Zn atoms[38]. The 2nd-nearest neighbors and bond angles,α,β, can be estimated by next equations[39, 40].

$$b_1' = c(1-u) \tag{11}$$

$$b_2' = \sqrt{a^2 + (uc)^2} \tag{12}$$

$$b_3' = \frac{4}{3}a^2 + c^2(\frac{1}{2} - u)^2 \tag{13}$$

$$\alpha = \frac{\pi}{2} + \cos^{-1}[1 + 3(\frac{c}{a})(-u + \frac{1}{2})^2]^{-\frac{1}{2}} \tag{14}$$

$$\beta = 2\sin^{-1}[\frac{4}{3} + 4(\frac{c}{a})^2(-u + \frac{1}{2})^2]^{-\frac{1}{2}} \tag{15}$$

The results obtained from the 2nd-nearest neighbours indicate that with an increase in cu ratio, the distance of the 2nd-nearest neighbours reduces. The values of b_1', b_2', b_3' bond angles,α,β, as a function of Cu ratio are summarized in table 3. An addition, from fig. 6, the positional parameter (u) and bond angle,β have a similar pattern, while the ratio,c/a and bond angle,α have the opposite tendency[40]. However, bond angle values show little variation from the value of the ideal ZnSe hexagonal phase. This could be owing to the difference in electro-negativity between the Cu and Zn atoms. Furthermore, the results reveal that substitutional Cu doping at Zn sites does not result in large-lattice distortion. As a consequence, the films under investigation are reasonable and practicable.[40, 41].

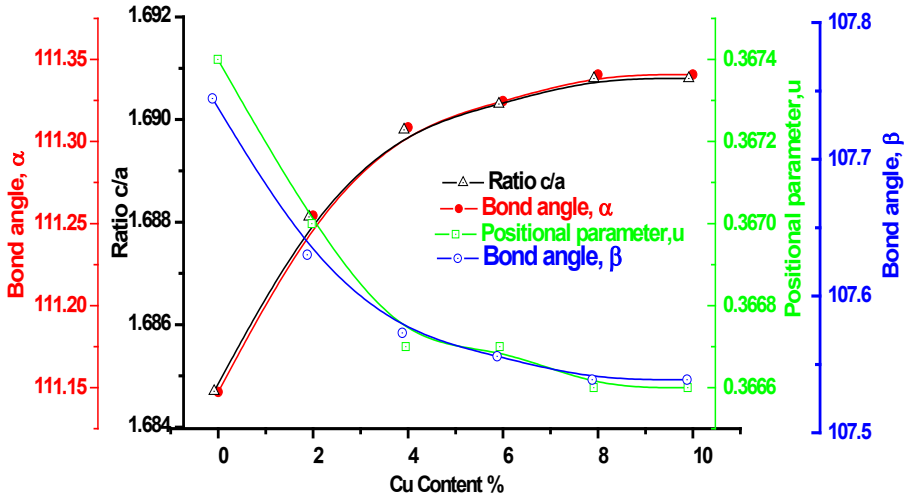

Fig. 6. Ratio c/a, positional parameter and bond angles,α,β, as a function of the Cu ratio.

Table 3. Some essential optical parameters which have been estimated for the polycrystalline films of Zn-Se-Cu matrix.

X%	E_d (eV)	E_o (eV)	M_1	M_3	ε_r	$N/m^* \times 10^{43}$ Kg^{-1}/m^{-3}	n_o	ε_i	$s_o \times 10^9$ m^2	λ_o nm
0	14.66	4.026	3.642	0.225	5.53	2.91	2.154	4.642	2.19	387.31
2	14.88	3.971	3.747	0.237	5.68	3.13	2.179	4.747	2.17	393.53
4	15.10	3.9217	3.853	0.25	5.84	3.36	2.203	4.853	2.158	399.24
6	15.35	3.8760	3.96	0.264	6.01	3.59	2.227	4.96	2.150	404.57
8	15.64	3.8615	4.051	0.272	6.13	3.73	2.247	5.051	2.11	406.21
10	15.98	3.8581	4.141	0.278	6.25	3.83	2.267	5.141	2.07	407.87

3.2. Optical analysis

3.2.1. Absorption coefficient and Refractive index

The optical parameters of the as-synthesized films $(ZnSe)_{1-x}Cu_x$ $(0 \leq x \leq 0.1)$ were investigated via spectrum values of reflectance, R_λ and transmittance, T_λ with a wavelength range of 300 to 2400 nm as presented in Fig. 7(a and b). From the figs. one can see, the absorption edge changes to a higher wavelength and occurs redshift of the absorption edge with increased Cu content.

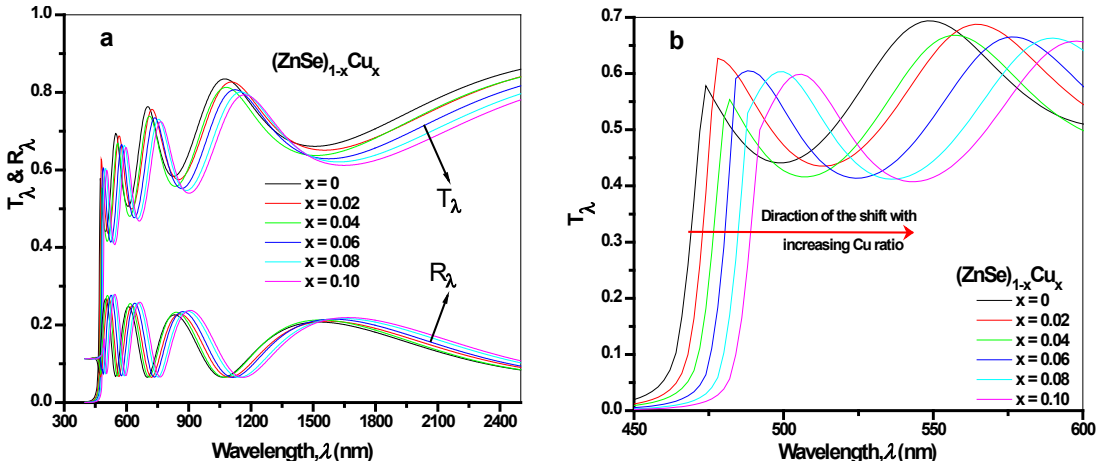

Fig. 7 a) The experimental values of the Reflectance,R_λ and Transmittance,T_λ with a wavelength of $(ZnSe)_{1-x}Cu_x$ $(0 \leq x \leq 0.1)$ thin films; b) The Transmittance,$T\lambda$ redshift of the absorption edge of $(ZnSe)_{1-x}Cu_x$ $(0 \leq x \leq 0.1)$ thin films.

This behaviors could be due to modifications in the structural characteristics and the enhancement of the crystallization process of the films as a result of the doped Cu atom within the ZnSe host crystalline lattice[8, 42]. On the other hand, the absorption data of films is regarding the essential absorption, that is, the transition from band-to-band. Thus, the absorption coefficient,α can be estimated according to the following expression[43, 44]

$$\alpha = \frac{1}{d}\ln\left[\frac{(1-R_\lambda)^2 + \sqrt{(1-R_\lambda)^4 + 4(T_\lambda R_\lambda)^2}}{2T_\lambda}\right] \tag{16}$$

where d is the film thickness, fig. 8 depicts the dependence of the absorption coefficient,α on photon energy,$h\upsilon$ of $(ZnSe)_{1-x}Cu_x$ $(0 \leq x \leq 0.1)$ films. It is observed that, the edge of absorption shifts towards lower photon energies,$h\upsilon$ as the Cu ratio increases, illustrating that the optical band gap,E_g^{opt} of the examined films is influenced by Cu content[45].

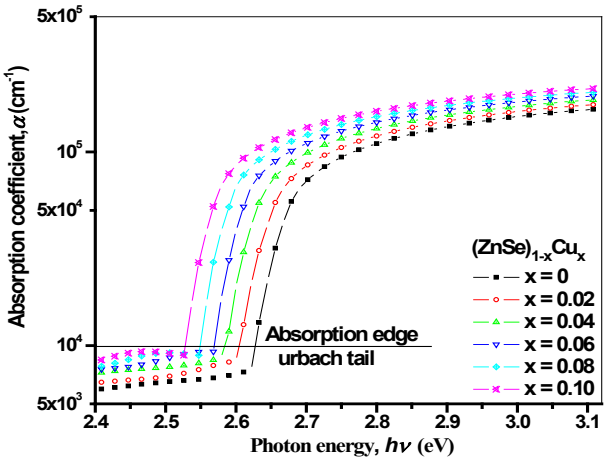

Fig. 8. The changes of absorption coefficient,α vs. the photon energy,hυ of (ZnSe)1-xCux (0 ≤ x ≤ 0.1) thin films.

To confirm the nature of optical transitions, we estimate the band gap,E_g^{opt} in the high absorption range($\alpha \geq 10^4$ cm^{-1}) via applying the Tauc-equation[46].

$$\alpha(h\upsilon) = \frac{B(h\upsilon - E_g^{opt})^r}{h\upsilon} \tag{17}$$

where B is a constant and r is the parameter that refers to the transition type of optical equal to ½ for the direct transitions that are allowed. In the current study the values of the optical band gap,E_g^{opt} can be obtained from the intersection of the straight lines at $(\alpha h\upsilon)^{1/2}=0$ as clear in Fig. 9. The obtained values of films under investigation are presented in fig 9.

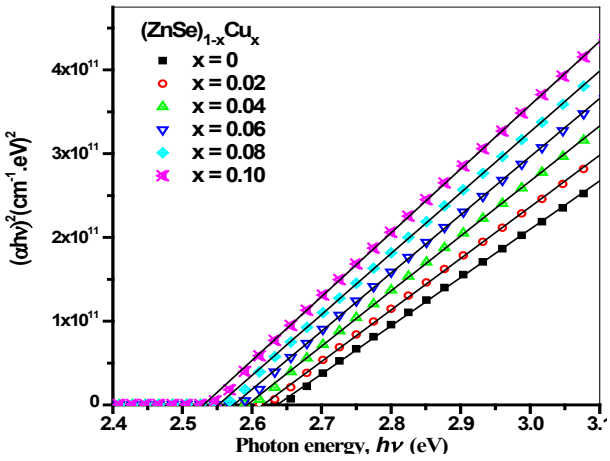

Fig. 9. The plotting of $(\alpha * h\upsilon)^2$ with photon energy,hυ of (ZnSe)1-xCux (0 ≤ x ≤ 0.1) thin films.

The results show that with increasing the Cu ratio the optical band gap,E_g^{opt} decreases from 2.63 eV to 2.52 eV (see fig. 11). This decrease could be related to defects which caused an Urbach tail, as a result of the formation of localized energy states near the band-edges leading to the adjustment of the optical band gap,E_g^{opt} in Zn-Se thin films with the incorporation of Cu atoms[47, 48]. In addition, the alteration in the optical band gap,E_g^{opt} indicates that there is direct

energy transfer between the semiconductor excited states and the 3^d levels of the Cu^{2+} ions via transfer energy processes[49, 50]. Moreover, near the edge of absorption spectra that the values of ($\alpha \leq 10^4$ cm) is corelating exponentially to the photon energy and known as Urbach tail state which calculated using the equation in the form[51].

$$\alpha(h\upsilon) = \alpha_0 \exp \frac{h\upsilon}{E_e} \tag{18}$$

where α_0 is a constant and E_e is the Urbach energy. By using this relation and plotting absorption coefficient ln (α) vs. photon energy,hυ as presented in fig. 10, the inverse of the straight line give the values of E_e. One can noticed that the values of E_e increase with increasing in Cu ratios due to generation of more defects and impurities in the localized states in conduction valence band edge. [51]. The values of E_e shown in as shown in fig (11)

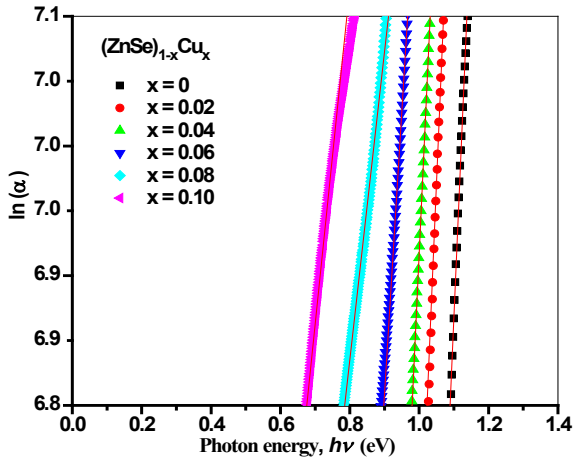

Fig. 10. Plot of the absorption coefficient ln(α) vs. photon energy(hυ) of pure ZnSe and doped with Cu ratio.

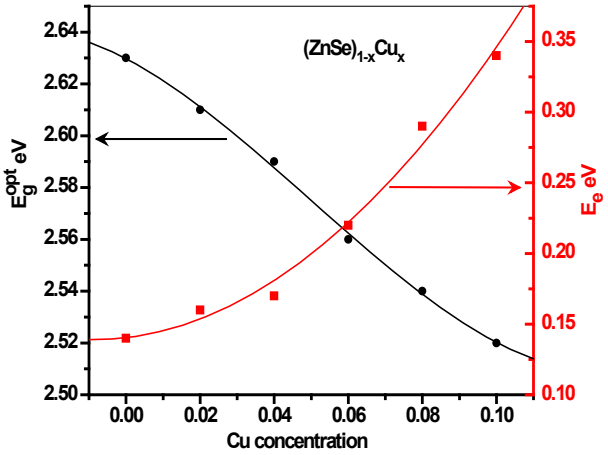

Fig. 11.The dependence of the optical band gap,E_g^{opt} and Urbach energy Ee on the variation of the Cu ratio.

It is noteworthy that, the parameters such as the refractive index,*n* and extinction coefficient,*k* are very interesting for opto-electronic devices applications. The refractive index,*n* of the current films under examination is estimated utilizing the envelope method that was suggested via Swanepoel[52, 53].

$$n = [N + (N^2 - s^2)^{1/2}]^{1/2} \tag{19}$$

where

$$N = 2s\frac{T_{Min} - T_{\min}}{T_{Min}T_{\min}} + \frac{s^2+1}{2} \quad , \quad s = \frac{1}{T_s} + (\frac{1}{T_s^2})^{1/2} \tag{20}$$

where T_{Min}, $T_{\min}$ are maxima and minima of the interference fringes, respectively and s is the refractive index of the substrate. According to the values of the estimated refractive index,*n* of $(ZnSe)_{1-x}Cu_x$ ($0 \le x \le 0.1$) films which are depicted in fig.12, it is found that the refractive index,n increases with the incorporation of Cu atoms in the host lattice.

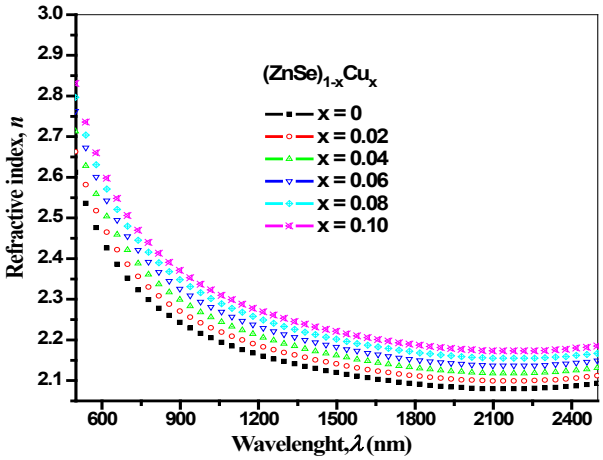

Fig. 12.The normal refractive index,n spectra of (ZnSe)1-xCux (0 ≤ x ≤ 0.1) thin films.

This behaviour may be related to the impurity-type scattering sites as a result of the enhancement of the number of atoms inside the interstitial network with an increase in Cu concentration. In other words, this is most likely connected to the alteration of the local field and ion polarizability into ZnSe lattice with the increasing Cu ratio in investigated films[7, 54]. Furthermore, the parameter of extinction coefficient,*k* of pure ZnSe and Cu-doped ZnSe thin films can be calculated based on the next eq.[55]

$$k = \frac{\alpha\lambda}{4\pi} \tag{21}$$

Fig.13 exhibits the variation of the extinction coefficient,*k* with the wavelength,λ. it is noticed that with an increased Cu ratio the values of *k* display a regular raise, while it reduced with an increase in the wavelength for all films under study at high absorption part of the spectra < 500 nm almost attend to zero values. This result may be attributed to structural instability or the emergence of point defects inside the lattice framework[49, 56].

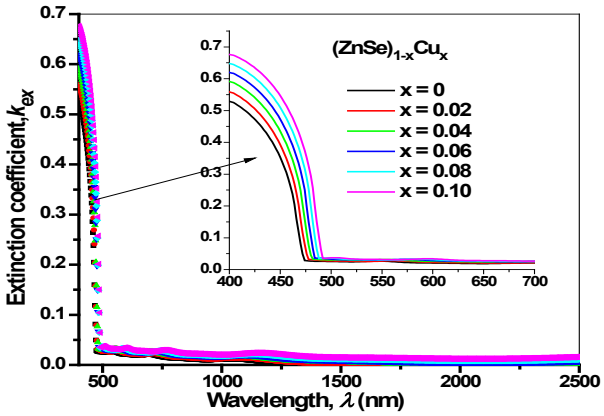

Fig. 13. The variation of extinction coefficient,k with the wavelength,λ of (ZnSe)1-xCux (0 ≤ x ≤ 0.1) thin films.

3.2.2. Dielectric constants and loss factor

The dielectric constant,($\varepsilon = \varepsilon_r + i\varepsilon_i$), is studying an substantial property of the material and are linked to *n* and *k*, the $\varepsilon_r = n^2 - k^2$ is the real part that refers to absence of energy or the imbibe light, while the $\varepsilon_i = 2nk$ expresses the imaginary part is known the damping factor, which gives the information about dissipative rate of energy through the propagation into the films and dissipation factor that is the ratio of the imaginary and real part tan $\delta = \varepsilon_i / \varepsilon_r$ [57]. The ε_r, ε_i and tan δ are determined for $(ZnSe)_{1-x}Cu_x$ ($0 \le x \le 0.1$) films and plotted with wavelength as a function the Zn ratio, showing in Fig. (14 a, b and c). The observed results indicate to the values of ε_r are heighted than those of ε_i and raise with rising Zn ratio.

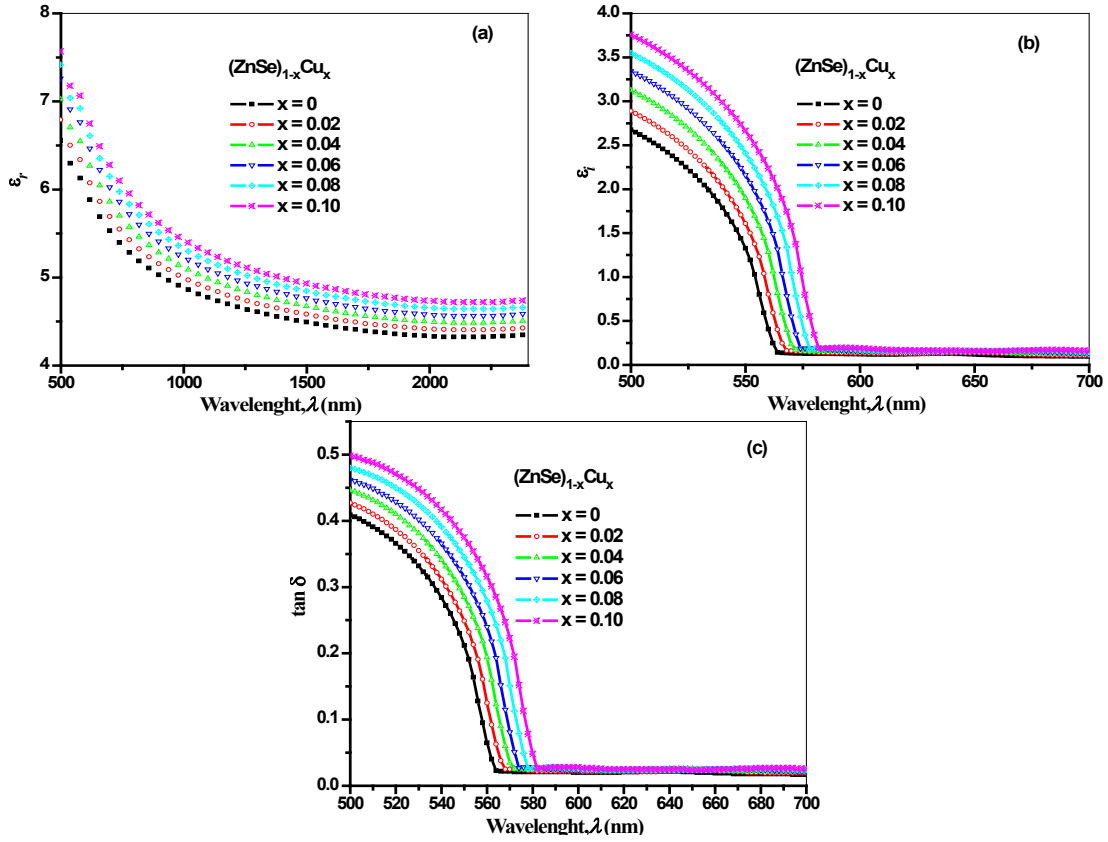

Fig. 14. Plots of real (a), imaginary (b) parts of the dielectric constants and dissipation factor tan δ (c) with the wavelength,λ of $(ZnSe)_{1-x}Cu_x$ ($0 \le x \le 0.1$) thin films.

There are anther two important parameters to understood how the energy absorption are loss and decelerated that occur during of single electron transitions or the collective effects that are induced into the solid. The loss of energy is represented by two functions the volume energy, (VELF) and surface energy loss functions (SELF), respectively, are related to the real,ε_r and imaginary,ε_i parts of the dielectric constants and deduced according the next eq.[49, 58].

$$VELF = \frac{\varepsilon_2}{\varepsilon_1^2 + \varepsilon_2^2} \quad \text{and} \quad SELF = \frac{\varepsilon_2}{(\varepsilon_1 + 1)^2 + \varepsilon_2^2} \tag{22}$$

The variations of the volume and surface energy loss functions (VELF and SELF) with of the photon energy,hν for poly-crystalline $(ZnSe)_{1-x}$ Cu_x thin films are illustrates in fig.(15 a and b). one can notice the values of function VELF and SELF respectively, rise with rising photon energy,hν and as well, one can notice the values of function VELF and SELF respectively, rise with rising photon energy,hυ and also, with increment the ratio of Cu into Zn-Se lattice both VELF and SELF are increases.

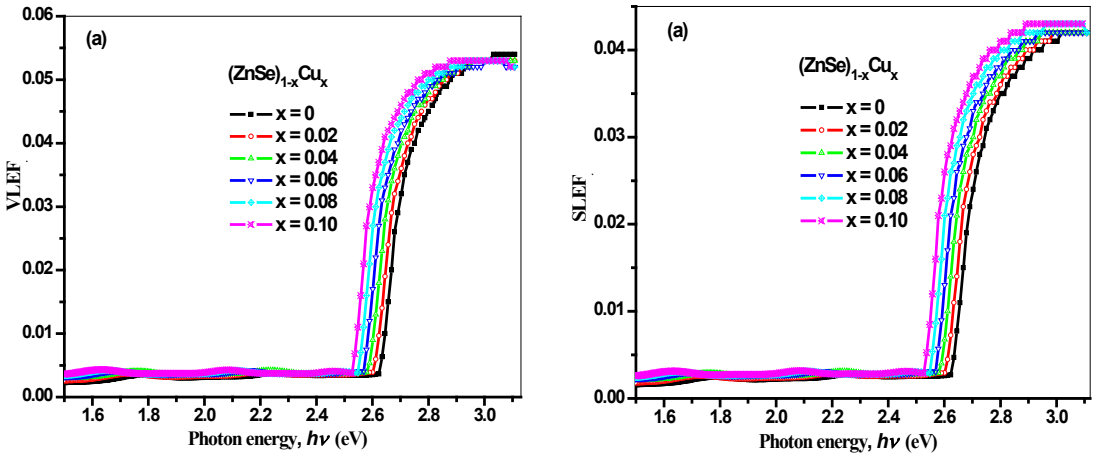

Fig. 15. The plots of VELF (a) and SELF (b) vs. photon energy(hυ) of $(ZnSe)_{1-x}Cu_x$ $(0 \le x \le 0.1)$ thin films.

Additionally, to acquire more understanding around optical reactions of the examined films. The optical conductivity,σ_{opt}, and electrical conductivity,σ_{elec} are considered of the powerful and important tools where these parameters provides details about the electronic state density within the material's bandgap and optical response and can be deduced by the absorption coefficient,α and refractive index,n based on the flowing eq. [59]:

$$\sigma_{opt.} = \alpha nc\varepsilon_o = \frac{\alpha nc}{4\pi} \quad \text{and} \quad \sigma_{elec.} = \left[\frac{2\lambda}{\alpha}\right].\sigma_{opt.} \tag{23}$$

where ε_0 is the electrical permittivity and c is the velocity of light. The dependence values of $\sigma_{opt.}$ and $\sigma elec.$ on photon energy, $h\upsilon$ are represented in fig.(16 a and b), the $\sigma opt.$ rises, while $\sigma elec.$ reduces with increasing photon energy,$h\upsilon$, this may be because of the strong excitement of the electrons and the higher absorbance of the films under studied. On the other hand, it is observed that with an increase the Cu ratio to Zn Se lattice both parameters of $\sigma_{opt.}$ and $\sigma elec.$ increase. This behaver are a good indication for utilizing the investigated films for opto-electronic applications[49].

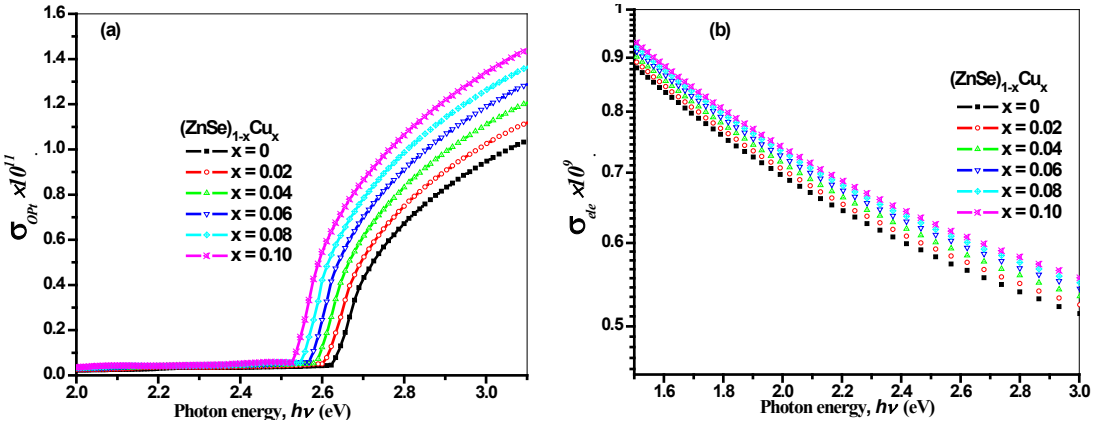

Fig. 16. Plots of optical conductivity,σ_{opt}, and electrical conductivity,σ_{elec} vs. photon energy, hυ of (ZnSe)1-xCux ($0 \le x \le 0.1$) thin films.

3.2.4. Dispersion parameters

The refractive index dispersion parameters are an essential factor used to indicate optoelectronic materials, which can be dissection using single oscillator model proposition by Wemple-DiDomenico [60].

$$n^2 = 1 + \left(\frac{E_o E_d}{E_o^2 - (h\upsilon)^2} \right) \tag{24}$$

where, E_o the single oscillator energy is contributed to the band structure of the materials and E_d is the dispersion energy explained the average energy and oscillator strength. Plotting and fitting of $(n^2 - 1)^{-1}$ vs. $(h\upsilon)^2$ as clearly in Fig (17) the straight line obtained. The E_d and E_o values were evaluated from the slope $(1/E_d E_o)$ and intercept (E_o/E_d) respectively.

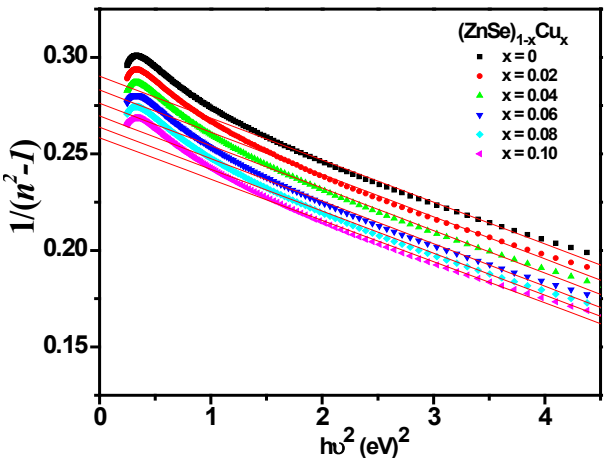

Fig. 17. Plots of $(n^2\text{-}1)^{-1}$ vs. $(h\upsilon)^2$ of (ZnSe)1-xCux ($0 \le x \le 0.1$) thin films.

The reduction values of E_o may be due to the strength of the optical inter-band transitions decreases with increasing the Cu ratio. The rises of E_d values could be attributed to the alteration in the atoms diffusion, referring to raise of the number of atoms at interstitial sites in the studied films[61]. the values E_o and E_d are listed in table (3). Other two optical parameters which called

the moments of the optical spectrum M_{-1} and M_{-3} contributed to the single oscillator energy,E_o and dispersion energy,E_d as described from the equation below

$$M_{-1} = \left(\frac{E_d}{E_o}\right) \quad \text{and} \quad M_{-3} = \left(\frac{M_{-3}}{E_o^2}\right) \tag{25}$$

The estimated values of M_{-1} and M_{-3} are listed in table (3). One can clearly notes the two moments are increased with increasing of Cu ratios.

Furthermore, in the real part of dielectric constant at high frequency it is of great importance by drawing square of refractive index,n^2 at a vertical axis versus the square of the wavelength,λ^2, the dielectric constant,ε_r is associated with free carrier concentration and can be estimated using the following relation [60]

$$n^2 = \varepsilon_r - \left(\frac{e^2 N}{4\pi c^2 \varepsilon_o m^*}\right)\lambda^2 \tag{26}$$

where e is the charge of electron and N is the conduction band free carrier concentration to the charge carrier effective mass m^* . Fig (18) shows the relation between (n^2) vs. λ^2, The value of ε_r equal the intercept of the straight line while the term of (N/m^*) were obtained from the slope of straight line, the determination values of ε_r and (N/m^*) listed in table (3).

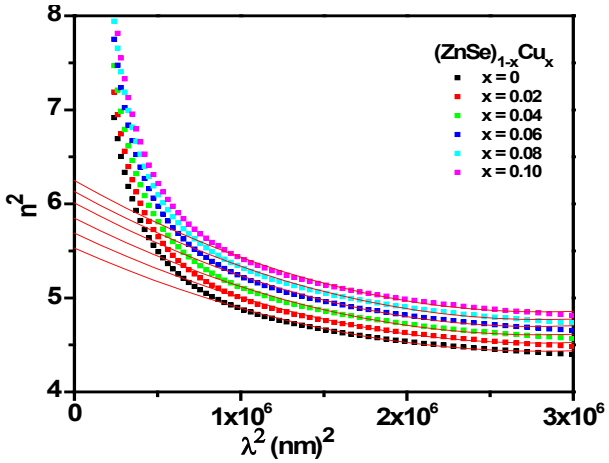

Fig. 18. Plots of n^2 vs. $(\lambda)^2$ of (ZnSe)1-xCux ($0 \le x \le 0.1$) thin films.

Moreover, the statistic refractive index,n_o is related to the effective oscillator model for ($h\upsilon = 0$) evaluated according to next equation.

$$n_o = \sqrt{1 + \frac{E_d}{E_o}} \tag{27}$$

Consequently, the values of zero-frequency dielectric constant $\varepsilon_i = n_o^2$ were conclude, the values of ε_r , (N/m^*), n_o and ε_i, increases directly with increasing the Cu ratios and $\varepsilon_i < \varepsilon_r$. This behaviour may be referred to the polarization process which occurs inner the material also, because of a rise of the free carrier concentration as resulted of the replacement of Cu^{2+} ions in the lattice matrix[62]. On the other hand, at low frequencies the oscillator wavelength,λ_0 and the oscillator strength,s_0 were deduced based on a Sellmeier oscillator function that describes below [63]

$$\frac{(n_\infty^2 - 1)}{(n^2 - 1)} = 1 - \left(\frac{\lambda_o}{\lambda}\right)^2 \tag{28}$$

The parameters (λ_o) and (s_o) for pure thin films ZnSe and dopant with Cu was evaluated from the slope and intercept of the straight line of the plots of $(n^2\text{-}1)^{-1}$ vs. λ^{-2} as shown in fig.(19). The estimated values of S_0 and λ_0 are listed in table (3). from this result the values of S_0 decrease with increasing in Cu ratios but λ_0 increases with increasing in Cu ratios. This means that the all parameters are dependent in the cu ratios[42, 64].

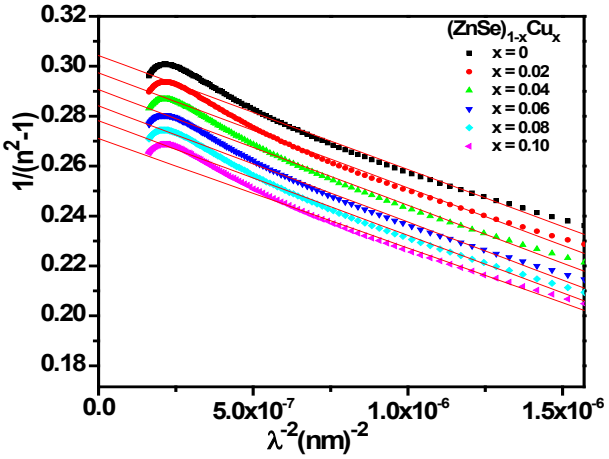

Fig. 19. The plot of $(n^2\text{-}1)^{-1}$ vs. λ^{-2} of (ZnSe)1-xCux ($0 \leq x \leq 0.1$) thin films.

4. Conclusion

The structural and optical characterization of $ZnSe)_{1-x}Cu_x$ ($0 \leq x \leq 0.1$) thin films which were synthesized using the "e-vaporation technique" have been studied. The analysis of structural results refers to the growth of a hexagonal wurtzite structure without the presence of any further phases. The results demonstrate that the micro-structural parameters enhancement with increment Cu atoms into the host Znse lattice, as a result of vacancies created with Cu substitution inside the ZnSe lattice, leads to lattice distortion. Likewise, the optical parameters of the as-synthesized films $(ZnSe)_{1-x}Cu_x$ ($0 \leq x \leq 0.1$) were performed utilising a "UV–V spectro-photometer" with a wavelength range of 300 to 2400 nm.

The results reveal nearly perfect optical transmittance (more than 80%). Also, the absorption edge changes to a higher wavelengths and there occurs a redshift of the absorption edge, confirming that Cu atoms doping in ZnSe causes a reduction in the optical energy gap,E_g^{opt}. Additionally, the optical constant parameters were shown to depend on the variation of the Cu ratio and wavelengths. Thus, as mentioned by the results, the incorporation of Cu atoms in the host lattice of ZnSe has a conclusive role in enhancement of the physical properties and holds promise for a wide range of technological photonic applications.

Acknowledgments

The authors extend their appreciation to the Deanship of Scientific Research at King Khalid University (KKU) for funding this research project Number (RGP2/431/44).

References

[1] P. Kumar, J. Singh, M.K. Pandey, C. Jeyanthi, R. Siddheswaran, M. Paulraj, K. Hui, K. Hui, Materials Research Bulletin, 49 (2014) 144-150; https://doi.org/10.1016/j.materresbull.2013.08.060

[2] E. Bacaksiz, S. Aksu, I. Polat, S. Yılmaz, M. Altunbaş, Journal of Alloys and Compounds, 487 (2009) 280-285; https://doi.org/10.1016/j.jallcom.2009.07.102

[3] Y. Deng, G. Chen, B. Pan, J. Li, G. Jiang, W. Liu, C. Zhu, Journal of alloys and compounds, 591 (2014) 117-120; https://doi.org/10.1016/j.jallcom.2013.12.073

[4] M. Frolov, Y.V. Korostelin, V. Kozlovsky, Y.P. Podmar'kov, Y.K. Skasyrsky, Optics letters, 43 (2018) 623-626; https://doi.org/10.1364/OL.43.000623

[5] E. Calderón-Ortiz, S. Bailón-Ruiz, M. Martínez-Ferrer, J. Rodríguez-Orengo, O. Perales-Pérez, Journal of Electronic Materials, 47 (2018) 4361-4365; https://doi.org/10.1007/s11664-018-6309-3

[6] X. Yang, C. Pu, H. Qin, S. Liu, Z. Xu, X. Peng, Journal of the American Chemical Society, 141 (2019) 2288-2298; https://doi.org/10.1021/jacs.8b08480

[7] G.A. Ali, M. Emam-Ismail, M. El-Hagary, E. Shaaban, S. Moustafa, M. Amer, H. Shaban, Optical Materials, 119 (2021) 111312; https://doi.org/10.1016/j.optmat.2021.111312

[8] M. Alzaid, N. Hadia, M. El-Hagary, E. Shaaban, W. Mohamed, Journal of Materials Science: Materials in Electronics, 32 (2021) 15095-15107; https://doi.org/10.1007/s10854-021-06061-8

[9] F. Yao, X. Zhou, A. Xiong, Applied Physics A, 126 (2020) 1-10; https://doi.org/10.1007/s00339-020-03674-4

[10] F. Long, S. Ning, W. Zhang, S. Wang, H. Yang, H. Zhang, G. Feng, S. Zhou, Laser Physics, 30 (2020) 055101; https://doi.org/10.1088/1555-6611/ab8233

[11] P. Zhou, M. Zhang, Q.H. Zhang, Z. Su, Y. Wang, X. Wang, Y. Hu, Y. Li, Z. Guo, Materials Letters, 273 (2020) 127945; https://doi.org/10.1016/j.matlet.2020.127945

[12] E. Molahossieni, M. Molaei, M. Karimipour, F. Amirian, Journal of Materials Science: Materials in Electronics, 31 (2020) 387-393; https://doi.org/10.1007/s10854-019-02537-w

[13] M.S. Khan, L. Shi, B. Zou, Computational Materials Science, 174 (2020) 109493; https://doi.org/10.1016/j.commatsci.2019.109493

[14] J. Yin, X. Zhang, Journal of Physics and Chemistry of Solids, 152 (2021) 109951; https://doi.org/10.1016/j.jpcs.2021.109951

[15] M. Alzaid, W. Mohamed, M. El-Hagary, E. Shaaban, N. Hadia, Optical Materials, 118 (2021) 111228; https://doi.org/10.1016/j.optmat.2021.111228

[16] Z.B. Bahşi, A.Y. Oral, Optical Materials, 29 (2007) 672-678; https://doi.org/10.1016/j.optmat.2005.11.016

[17] T. Kutty, N. Raghu, Applied physics letters, 54 (1989) 1796-1798; https://doi.org/10.1063/1.101267

[18] H. Katagiri, N. Sasaguchi, S. Hando, S. Hoshino, J. Ohashi, T. Yokota, Solar Energy Materials and Solar Cells, 49 (1997) 407-414; https://doi.org/10.1016/S0927-0248(97)00119-0

[19] M. El Sherif, F. Terra, S. Khodier, Journal of Materials Science: Materials in Electronics, 7 (1996) 391-395; https://doi.org/10.1007/BF00180775

[20] W. Daranfed, M.S. Aida, N. Attaf, J. Bougdira, H. Rinnert, Journal of alloys and compounds, 542 (2012) 22-27; https://doi.org/10.1016/j.jallcom.2012.07.063

[21] J.-S. Seol, S.-Y. Lee, J.-C. Lee, H.-D. Nam, K.-H. Kim, Solar Energy Materials and Solar Cells, 75 (2003) 155-162; https://doi.org/10.1016/S0927-0248(02)00127-7

[22] A. Rumberg, C. Sommerhalter, M. Toplak, A. Jäger-Waldau, M.C. Lux-Steiner, Thin Solid Films, 361 (2000) 172-176; https://doi.org/10.1016/S0040-6090(99)00790-7

[23] Korneeva., Sov. Phys. Crystallogr. (Engl. Transl.), 6, 505, (1962).

[24] D. Hile, H. Swart, S. Motloung, T. Motaung, R. Kroon, K. Egbo, V. Pawade, L. Koao, Materials Chemistry and Physics, 262 (2021) 124303; https://doi.org/10.1016/j.matchemphys.2021.124303

[25] S. Syed Zahirullah, J. Joseph Prince, P. Fermi Hilbert Inbaraj, Materials technology, 32 (2017) 755-763; https://doi.org/10.1080/10667857.2017.1351656

[26] P.H. Lee, S. Brahma, J. Dutta, J.-L. Huang, C.-P. Liu, Nanoscale Advances, 3 (2021) 3909-3917; https://doi.org/10.1039/D0NA01069C

[27] D.D. Hile, H.C. Swart, S.V. Motloung, T.E. Motaung, L.F. Koao, Physica B: Condensed Matter, 575 (2019) 411706; https://doi.org/10.1016/j.physb.2019.411706

[28] D. Hile, H. Swart, S. Motloung, T. Motaung, K. Egbo, L. Koao, Superlattices and Microstructures, 134 (2019) 106222; https://doi.org/10.1016/j.spmi.2019.106222

[29] L.P. Deshmukh, P.C. Pingale, S.S. Kamble, N.N. Maldar, Composites Part B: Engineering, 85 (2016) 286-293; https://doi.org/10.1016/j.compositesb.2015.09.047

[30] S. Thakur, N. Sharma, A. Varkia, J. Kumar, Advances in Applied Science Research, 5 (2014) 18-24.

[31] M. Emam-Ismail, M. El-Hagary, E. Shaaban, S. Althoyaib, Journal of alloys and compounds, 529 (2012) 113-121; https://doi.org/10.1016/j.jallcom.2012.03.027

[32] A.J.C. Wilson, Mathematical theory of X-ray powder diffractometry, Centrex Publishing Company, 1963.

[33] M. Dhanam, R. Balasundaraprabhu, S. Jayakumar, P. Gopalakrishnan, M. Kannan, Physica Status Solidi A, 191 (2002) 149-160; https://doi.org/10.1002/1521-396X(200205)191:1<149::AID-PSSA149>3.0.CO;2-F

[34] E.R. Shaaban, M. Mohamed, M.N. Abd-el Salam, A.Y. Abdel-Latief, M.A. Abdel-Rahim, E.S. Yousef, Optical Materials, 86 (2018) 318-325; https://doi.org/10.1016/j.optmat.2018.10.027

[35] M. Amer, S. Moustafa, M. El-Hagary, Materials Chemistry and Physics, 248 (2020) 122892; https://doi.org/10.1016/j.matchemphys.2020.122892

[36] D. Dwivedi, N. Shukla, H. Pathak, K. Singh, American Journal of Materials Science and Engineering, 2 (2014) 13-17; https://doi.org/10.12691/ajmse-2-2-1

[37] X. Wang, Z. Wu, J. Webb, Z. Liu, Applied Physics A, 77 (2003) 561-565; https://doi.org/10.1007/s00339-002-1497-2

[38] M. Alzaid, A. Qasem, E. R. Shaaban, N. M. A. Hadia, Optical Materials 110 (2020) 110539; https://doi.org/10.1016/j.optmat.2020.110539

[39] L. Bruno Chandrasekar, R. Chandramohan, S. Chandrasekaran, J. Thirumalai, R. Vijayalakshmi, Advanced Science Focus, 1 (2013) 292; https://doi.org/10.1166/asfo.2013.1047

[40] M.N.H. Mia, M.F. Pervez, M.K. Hossain, M.R. Rahman, M.J. Uddin, M.A. Al Mashud, H.K. Ghosh, M. Hoq, Results in physics, 7 (2017) 2683-2691; https://doi.org/10.1016/j.rinp.2017.07.047

[41] Y. Zhang, G. Feng, S. Dai, S. Ning, S. Zhou, Physica Status Solidi B, 253 (2016) 1133-1137; https://doi.org/10.1002/pssb.201552684

[42] A.S. Hassanien, R. Neffati, K. Aly, Optik, 212 (2020) 164681; https://doi.org/10.1016/j.ijleo.2020.164681

[43] R. Vahalová, L. Tichý, M. Vlček, H. Tichá, Physica Status Solidi A 181(2000) 199-209; https://doi.org/10.1002/1521-396X(200009)181:1<199::AID-PSSA199>3.0.CO;2-X

[44] E.R. Shaaban, M.N. Abd-el Salam, M. Mohamed, M.A. Abdel-Rahim, A.Y. Abdel-Latief, Journal of Materials Science: Materials in Electronics, 28 (2017) 13379-13390; https://doi.org/10.1007/s10854-017-7175-0

[45] M. Alzaid, M. Alwshih, M.N. Abd-el Salam, N. Hadia, Materials Science in Semiconductor Processing, 127 (2021) 105687; https://doi.org/10.1016/j.mssp.2021.105687

[46] J. Tauc, Amorphous and liquid semiconductors, Plenum Press, New York (1974); https://doi.org/10.1007/978-1-4615-8705-7

[47] R. Panda, V. Rathore, M. Rathore, V. Shelke, N. Badera, L.S. Sharath Chandra, D. Jain, M. Gangrade, T. Shripati, V. Ganesan, Applied Surface Science, 258 (2012) 5086-5093; https://doi.org/10.1016/j.apsusc.2012.01.131

[48] E. R. Shaaban, M. S. Abd El-Sadek, M. El-Hagary, I. S Yahia, Physica Scripta 86 (1) (2012)

015702; **https://doi.org**/10.1088/0031-8949/86/01/015702

[49] M. Mohamed, A. Abdelraheem, M. Abd-Elrahman, N. Hadia, E. Shaaban, Applied Physics A, 125 (2019) 483; https://doi.org/10.1007/s00339-019-2774-7

[50] F.J. Brieler, M. Froeba, L. Chen, P.J. Klar, W. Heimbrodt, H.-A. Krug von Nidda, A. Loidl, ChemInform ChemInform, 33 (2002); https://doi.org/10.1002/chin.200219011

[51] E.R. Shaaban, M.M. Soraya, M. Shapaan, H.S. Hassan, M.M. Samar, Journal of Alloys and Compounds, 693 (2017) 1052-1060; https://doi.org/10.1016/j.jallcom.2016.09.264

[52] R. Swanepoel, Journal of Physics E: Scientific Instruments, 17 (1984) 896- 903; https://doi.org/10.1088/0022-3735/17/10/023

[53] R. Swanepoel, Journal of Physics E: Scientific Instruments, 16 (1983), 1214- 1222; https://doi.org/10.1088/0022-3735/16/12/023

[54] S. Li, L. Wang, X. Su, Y. Pan, D. Gao, X. Han, Thin Solid Films, 692 (2019) 137599; https://doi.org/10.1016/j.tsf.2019.137599

[55] M. El-Hagary, M. Emam-Ismail, E. Shaaban, A. Al-Rashidi, S. Althoyaib, Materials Chemistry and Physics, 132 (2012) 581-590; https://doi.org/10.1016/j.matchemphys.2011.11.072

[56] A.A. Aboud, A. Mukherjee, N. Revaprasadu, A.N. Mohamed, Journal of Materials Research and Technology, 8 (2019) 2021-2030; https://doi.org/10.1016/j.jmrt.2018.10.017

[57] D. Prakash, A. M. Aboraia, M. El-Hagary, E. R. Shaaban, K. D. Verma, Ceramics International 42 (2) (2016) 2676-2685; https://doi.org/10.1016/j.ceramint.2015.10.096

[58] S. Wemple, Physical Review B, 7 (1973) 3767; https://doi.org/10.1103/PhysRevB.7.3767

[59] J.I. Pankove, Optical Processes in Semiconductors, Courier Corporation, New York, 1975.

[60] S. H. Wemple, DiDomenico, Physical Review B, 3 (1971) 1338 – 1351; https://doi.org/10.1103/PhysRevB.3.1338

[61] Y. Jung, O. Güneş, G. Belev, C. Koughia, R. Johanson, S. Kasap, Journal of Materials Science: Materials in Electronics, (2017) 1-12; https://doi.org/10.1007/s10854-017-6550-1

[62] Mansour Mohamed, A. M. Abdelraheem, M. I. Abd-Elrahman, N. M. A. Hadia, E.R. Shaaban, Applied Physics A (2019) 125:483; https://doi.org/10.1007/s00339-019-2774-7

[63] A. Walton, T. Moss, Proceedings of the physical Society, 81 (1963) 509; https://doi.org/10.1088/0370-1328/81/3/319

[64] M. Hasaneen, Z. Alrowaili, W. Mohamed, Materials Research Express, 7 (2020) 016422; https://doi.org/10.1088/2053-1591/ab6779